Modulational instability in one-dimensional saturable waveguide arrays: Comparison with Kerr nonlinearity

Milutin Stepić [a,b,*], Christian E. Rüter [a], Detlef Kip [a], Aleksandra Maluckov [c], Ljupčo Hadžievski [b]

[a] *Institute of Physics and Physical Technologies, Clausthal University of Technology, Leibnizstraße 4, D-38678 Clausthal-Zellerfeld, Germany*
[b] *Vinča Institute of Nuclear Sciences, P.O. Box 522, 11001 Belgrade, Serbia and Montenegro*
[c] *Faculty of Sciences and Mathematics, Department of Physics, P.O. Box 224, 18001 Niš, Serbia and Montenegro*

Abstract

Discrete modulational instability within the first band of uniform one-dimensional waveguide arrays possessing a saturable self-defocusing nonlinearity is investigated in detail within the coupled mode approach. Explicit analytical results for both the threshold and the maximal gain of instability are compared with the corresponding data from waveguide arrays exhibiting Kerr nonlinearity. We find that saturation bounds the interval of existence of discrete modulational instability, stabilizes the frequency region of perturbations around $\pm\pi/2$ and decreases both gain and critical spatial frequency of perturbations.
© 2006 Elsevier B.V. All rights reserved.

1. Introduction

Modulational instability (MI) is a universal process in which tiny phase and amplitude perturbations that are always present in a wide input beam grow exponentially during propagation under the interplay between diffraction (in spatial domain) or dispersion (in temporal domain) and nonlinearity. This process has been observed in various nonlinear systems such as auroral ionosphere [1], magneto-static waves [2], globular proteins [3], two-dimensional lattices [4], or Bose–Einstein condensates [5]. In nonlinear optics, MI has been studied in lossy fibers [6], fiber gratings [7], for incoherent light [8], and second har-

monic generation [9], to mention a few. Furthermore, this phenomenon is investigated in media with different type of the nonlinear response such as integrating [10], nonlocal [11], quadratic [12], cubic-quintic [13], varying [14], and saturable one [15,16].

Nonlinear waveguide arrays (NWA's) represent arrays of aligned channel waveguides which are close enough to allow for tunnelling of energy from one channel to its neighbors. It has been demonstrated that such systems can be implemented in various all-optical devices [17–22]. The NWA's can be either uniform [23–26] with a fixed distance between the channels of equal shape, modulated [19], or nonuniform [18,22]. A uniform NWA is a periodic system with corresponding Floquet–Bloch modes and band-gap structure. Within the first band the beam dynamics can be well described by virtue of a coupled mode approach [21,27,28].

Discrete MI was proposed for uniform NWA with cubic (Kerr) nonlinearity [24]. Thereafter, theoretical

---

* Corresponding author. Address: Institute of Physics and Physical Technologies, Clausthal University of Technology, Leibnizstraße 4, D-38678 Clausthal-Zellerfeld, Germany. Tel.: +49 5323 72 2282; fax: +49 5323 72 2175.
E-mail address: milutin.stepic@tu-clausthal.de (M. Stepić).

investigations of this process have been performed in re-orientable [29] and saturable discrete media [30,31]. Experimentally, discrete MI was observed in cubic aluminium gallium arsenide (AlGaAs) [27], in photorefractive strontium–barium niobate (SBN) [28], and in lithium niobate (LN) [32,33].

For both, semiconductor and photorefractive materials, it is well known that the optically induced refractive index change Δn becomes saturated at moderately high field strengths [34]. The purpose of this paper is to investigate in which way the effect of saturation modifies the MI behavior of NWA's. As powers required to observe nonlinear effects in AlGaAs and LN differ by a few orders of magnitude [27,32], we reduce the model equations to the nondimensional forms in Section 2. By taking into account currently available experimental data we restrict the parameter space (i.e., coupling and nonlinear coefficient) to the region where this comparison can be made. Explicit results for the corresponding dispersion relation, gain, and critical spatial frequency of small perturbations are given altogether in this Section. Section 3 is devoted to a discussion of the obtained results. Conclusions are drawn in the last section.

2. Model equations

According to Ref. [25], optical beam propagation in uniform one-dimensional (1D) NWA's with self-defocusing Kerr nonlinearity can be described by a set of linearly coupled nonlinear ordinary differential equations:

$$i\frac{dE_n}{dz} + C_K(E_{n+1} + E_{n-1} - 2E_n) - \beta_K|E_n|^2 E_n = 0. \tag{1}$$

The propagation coordinate is denoted by z, E_n is the electric field of the nth element of the array, C_K is the coupling coefficient, while $\beta_K = w_0 n_2/cA_{\text{eff}} > 0$ represents the nonlinear coefficient due to the Kerr effect. Here w_0 is the circular frequency, c is the speed of light, A_{eff} is the effective cross-sectional area of a single waveguide, whereas n_2 represents the Kerr coefficient. The effect of self-defocusing is observed in various materials such as semiconductor doped glasses [35], ethanol solutions of Japanese green tea [36], and lead zirconate titanate [37]. Both Y junctions and bright temporal solitons are observed in such media [38,39].

Assuming a stationary solution of this equation in the form $E_n = E_0\exp[i(-qz + n\pi)]$, one can get the following dispersion relation: $q = 4C_k + \beta_K|E_0|^2$. The amplitude of this uniform staggered solution, where adjacent elements of the array are out of phase, is given by:

$$E_0 = \sqrt{\frac{q - 4C_K}{\beta_K}}. \tag{2}$$

This solution exists if $q > 4C_K$.

On the other hand, by taking into account the effect of saturation [15,16,40], one can describe beam propagation in a self-defocusing 1D NWA with the following set of difference-differential equations [31]:

$$i\frac{dE_n}{dz} + C_S(E_{n+1} + E_{n-1} - 2E_n) - \beta_S\frac{|E_n|^2 E_n}{|E_d|^2 + |E_n|^2} = 0. \tag{3}$$

Here E_d is the dark electrical field while $\beta_S > 0$ represents the corresponding nonlinear coefficient. Now, the above mentioned stationary solution has a dispersion relation of the form $q = 4C_S + \beta_S|E_0|^2(|E_0|^2 + |E_d|^2)^{-1}$ with amplitude

$$E_0 = \sqrt{\frac{q - 4C_S}{\beta_S - (q - 4C_S)}|E_d|^2}. \tag{4}$$

Contrary to the Kerr case, here we have a *bounded* domain of existence: $4C_S \leqslant q \leqslant \beta_S + 4C_S$.

The perturbed solution $[E_0 + \delta_n(z)]\exp[i(-qz + n\pi)]$, where $|\delta_n| \ll E_0$, satisfies the corresponding difference-differential equation

$$i\frac{d\delta_n}{dz} - C_K(\delta_{n+1} + \delta_{n-1} - 2\delta_n) - \beta_K|E_0|^2(\delta_n + \delta_n^*) = 0 \tag{5}$$

in cubic NWA, and

$$i\frac{d\delta_n}{dz} - C_S(\delta_{n+1} + \delta_{n-1} - 2\delta_n) - \beta_S\frac{|E_0|^2}{|E_d|^2 + |E_0|^2}$$
$$\times \left(1 - \frac{|E_0|^2}{|E_d|^2 + |E_0|^2}\right)(\delta_n + \delta_n^*) = 0 \tag{6}$$

in NWA with saturable nonlinearity.

The linear stability of a uniform solution has been investigated with different forms of perturbations [23,24,30]. Here, we adopt the perturbation form from Ref. [23]: $\delta_n = \epsilon_1 \exp[i(Qz - n\Omega D)] + \epsilon_2 \exp[-i(Qz - n\Omega D)]$, in which $\epsilon_{1,2}$ are constants while Q and Ω are parameters of a modulated wave. After a straightforward calculation one obtains the following expressions for the MI gain ($Q = \text{Im}\Gamma$):

$$\Gamma_K = \pm2\sqrt{2C_K}\sin(\Omega D/2)\sqrt{\beta_K E_0^2 - 2C_K\sin^2(\Omega D/2)} \tag{7}$$

in Kerr case, and

$$\Gamma_S = \pm2\sqrt{2C_S}\sin(\Omega D/2)$$
$$\times \sqrt{\beta_S\frac{|E_0|^2}{|E_d|^2 + |E_0|^2}\left(1 - \frac{|E_0|^2}{|E_d|^2 + |E_0|^2}\right) - 2C_S\sin^2(\Omega D/2)} \tag{8}$$

in saturable case. Instability occurs if $\Gamma_{K,S} > 0$, which is fulfilled for $0 < \Omega < 2\pi D^{-1}$. All uniform waves with wave numbers from this interval will be unstable if the input intensity exceeds the critical (threshold) value, i.e. for the case where the (saturable) nonlinearity exceeds linear diffraction effects. In cubic NWA's this value reads:

$$|E_0|^2 \geqslant (|E_0|^2)_{\text{cr}} = \frac{2C_K}{\beta_K}\sin^2(\Omega D/2). \tag{9}$$

In saturable NWA's uniform staggered waves exist only in a limited interval. Therefore, the MI region is bounded from both below and above:

$$\frac{1 - \sqrt{1 - \frac{8C_S}{\beta_S}\sin^2(\Omega D/2)}}{1 + \sqrt{1 - \frac{8C_S}{\beta_S}\sin^2(\Omega D/2)}}|E_d|^2$$

$$\leqslant |E_0|^2 \leqslant \frac{1 + \sqrt{1 - \frac{8C_S}{\beta_S}\sin^2(\Omega D/2)}}{1 - \sqrt{1 - \frac{8C_S}{\beta_S}\sin^2(\Omega D/2)}}|E_d|^2. \qquad (10)$$

Maximal gain (determined from the condition $\partial\Gamma_{K,S}/\partial\Omega = 0$) can be achieved in both cases if $\Omega^{\max} = 2\pi D^{-1}(m + 0.5)$, where m is an integer. Additionally, maximal gain appears for

$$\Omega_K^{\max} = \frac{2}{D}\arcsin\left(\pm\sqrt{\frac{\beta_K|E_0|^2}{4C_K}}\right) \qquad (11)$$

in Kerr case, and

$$\Omega_S^{\max} = \frac{2}{D}\arcsin\left(\pm\sqrt{\frac{\beta_S}{4C_S}\frac{|E_0|^2}{|E_d|^2 + |E_0|^2}\left(1 - \frac{|E_0|^2}{|E_d|^2 + |E_0|^2}\right)}\right) \qquad (12)$$

in saturable case. The maximal gain is given by

$$\Gamma_K^{\max} = \beta_K|E_0|^2, \quad \Gamma_S^{\max} = \beta_S\frac{|E_0|^2}{|E_d|^2 + |E_0|^2}\left(1 - \frac{|E_0|^2}{|E_d|^2 + |E_0|^2}\right), \qquad (13)$$

respectively.

To concretize these results we restrict our general considerations of NWA's to the semiconductor AlGaAs and photovoltaic LN crystals. AlGaAs is sensitive in the infrared part of the spectrum while the usual laser power necessary to excite reasonable nonlinear effects in NWA is in the range of hundreds of watts. The refractive index n_r of AlGaAs depends on composition and varies between 3.4 and 3.5 [27,41]. The Kerr coefficient for this material is approximately $n_2 = 2 \times 10^{-17}$ m^2 W^{-1} [27,39]. On the other hand, LN is sensitive in the visible part of the spectrum (blue–green wavelengths) and the required laser power is of the order of microwatts [32,42]. Here, the (extraordinary) refractive index for green light of $\lambda = 514.5$ nm is $n_r = 2.242$. In order to realize the influence of different forms of the nonlinear term in Eqs. (1) and (3) we have reduced the model equations to a nondimensional form. The propagation coordinate is now $\xi_{K,S} = z/(k_{K,S}x_0^2)$, where $k_{K,S} = 2\pi n_{rK,S}/\lambda_{K,S}$ and x_0 is an arbitrary length. We choose $x_0 = 10$ μm, which is of the order of a typical lattice period. The normalized distance between the centers of adjacent elements is $\widetilde{D} = D/x_0$. The coupling constants and nonlinear coefficients are multiplied with the belonging factor $k_{K,S}x_0^2$. The nondimensional variables are $U_n = E_n/\sqrt{P}$ and $U_n = E_n/E_d$, respectively, where P is light power. All above mentioned results on dispersion relation,

MI gain, and maximal frequency of perturbations are valid. It is only necessary to perform the following substitutions: $z \to \xi$, $E_n \to U_n$, $E_0 \to U_0$, $|E_d|^2 \to 1$, $D \to \widetilde{D}$, $C_{K,S} \to \widetilde{C}_{K,S}$, and $\beta_{K,S} \to \widetilde{\beta}_{K,S}$.

Finally, it is necessary to determine the realistic joint parameter range. With $x_0 = 10$ μm the usual normalized distance is in the range $[0.5, 2]$ [27,28,32]. Experimentally reported values for the coupling constants in the two materials are typically less than 2 mm^{-1} [27,32]. Thus the corresponding dimensionless coupling constants are in the range of 1. For waveguide cross sections A_{eff} as low as 10 μm^2 the nonlinear coefficient in AlGaAs can be estimated to be less than 10 m^{-1} W^{-1} With typical maximum input powers per channel that are of the order of 1 kW [27], normalized values of the coupling constant are in the range $[0, 30]$. The nonlinearity in LN crystals originates from the internal photovoltaic field that can be additionally enhanced by a suitable doping process [43]. Samples with a nonlinear coefficient up to 15 mm^{-1} have been fabricated; this value corresponds to a nonlinear refractive index change of $\Delta n_{\max} = 7 \times 10^{-4}$ (see Fig. 4 in Ref. [42]). Here, normalized values of the nonlinear coefficient lie in $[0, 40]$. In what follows we choose the following set of coupling constants $C \in \{0.5, 1.5, 2.5\}$ and nonlinear coefficients $\beta \in \{5, 10, 15, 20, 25\}$ (we dropped out $\sim$ for the sake of the simplicity). All
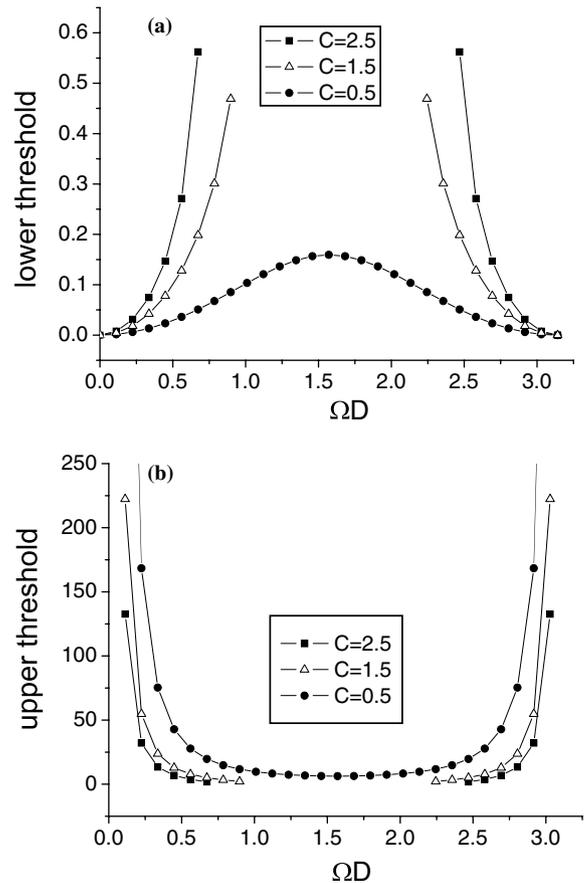

Fig. 1. Threshold behavior of discrete MI in saturable nonlinear media: dependence of (a) lower and (b) upper threshold on the spatial frequency of the perturbation for $\beta = 15$ and different values of coupling constants.

results are given for uniform arrays consisting of 28 channels with a corresponding normalized distance equal to 0.76.

3. Discussion

Firstly, we have investigated in which way the parameters of the discrete saturable system influence the lower and the upper threshold for the onset of MI that are given by Eq. (10). The lower threshold increases with stronger coupling while the upper one decreases, as illustrated in Fig. 1a and b, respectively. Due to symmetry, only the positive frequency region is presented. Furthermore, the frequency region around $\pm\pi/2$ becomes modulationally stable and broadens with increase of C. Therefore, with the nonlinearity fixed, stronger coupling has an inhibiting influence on MI. On the other hand, for fixed coupling, an enhancement of the nonlinearity leads to a drop of the lower threshold (Fig. 2a) and to a growth of the upper one (Fig. 2b). Additionally, stronger nonlinearity causes a destabilization of the frequency region around $\pm\pi/2$. Thus, an increase of nonlinearity has a catalytic role on the MI
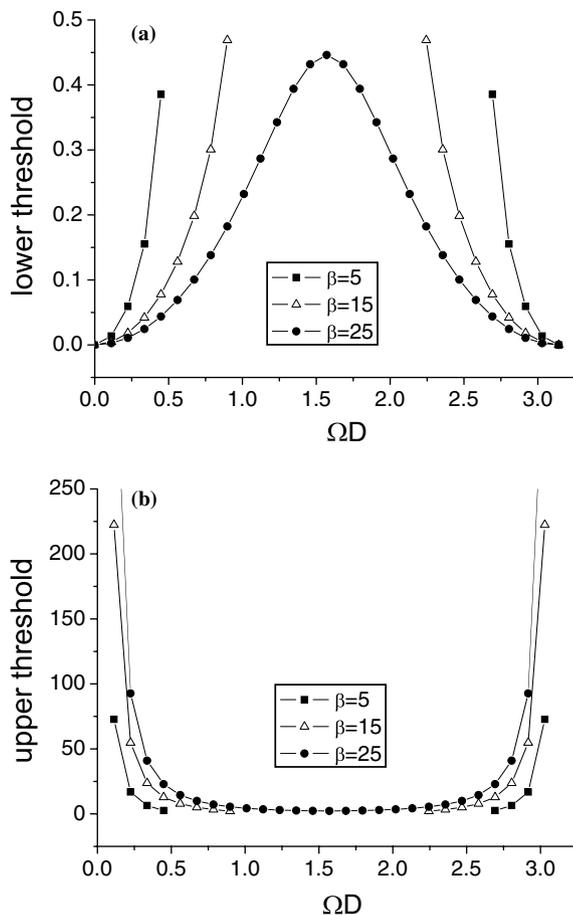
process. The same is true for the single threshold within the Kerr model [25].

One may notice in Fig. 3a and b that, for fixed values of the nonlinear coefficient and beam amplitude, stronger coupling decreases the critical spatial frequency that is given by Eqs. (11) and (12). Physically, stronger coupling results in broader products of MI (discrete solitons), independently of the type of nonlinearity. Consequently, the number of these localized structures per given array (i.e., spatial frequency) decreases. In the Kerr case of AlGaAs (Fig. 3a) there exists an unique critical spatial frequency that can be obtained for different values of beam amplitude and coupling constant (i.e., stronger coupling requires higher amplitudes). On the contrary, for saturable LN NWA's (Fig. 3b) there are different critical spatial frequencies which have the same amplitude and whose values decrease with stronger coupling.

In Fig. 4a and b the dependence of the critical spatial frequency on the beam amplitude is presented for different values of nonlinearity, whereas both the distance between waveguides and the coupling coefficient are fixed. The fact that magnification of the nonlinearity increases the critical spatial frequency can be easily explained as follows: A stronger nonlinearity of the system leads to a larger number of very narrow strongly localized modes in discrete MI.

Fig. 2. Threshold behavior of discrete MI in saturable nonlinear media: dependence of (a) lower and (b) upper threshold on the spatial frequency of the perturbation for $C = 1.5$ and different values of nonlinear coefficients.
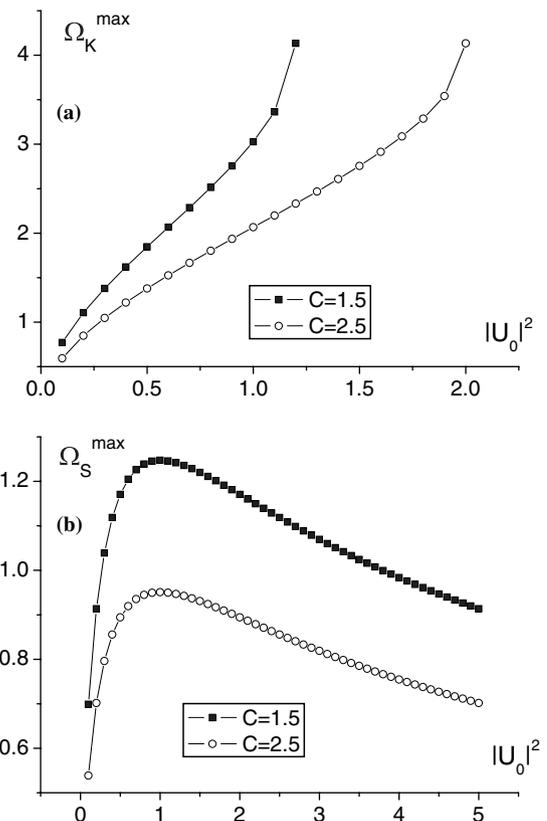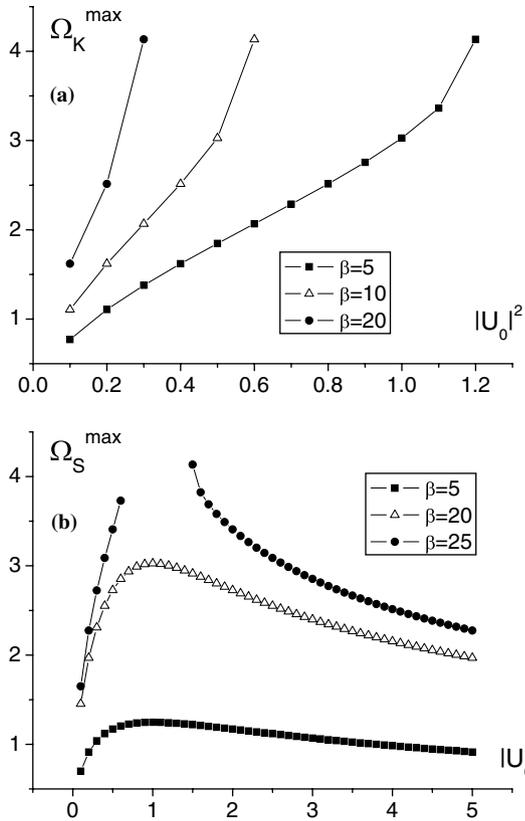

Fig. 3. Critical spatial frequency as a function of the square of the normalized wave amplitude in (a) Kerr and (b) saturable case. Normalized distance between waveguides is $D = 0.76$, while nonlinear coefficient is $\beta = 5$.

Fig. 4. Critical spatial frequency as a function of the square of the normalized wave amplitude in (a) Kerr and (b) saturable case. Normalized distance between waveguides is $D = 0.76$, while coupling constant is $C = 1.5$.
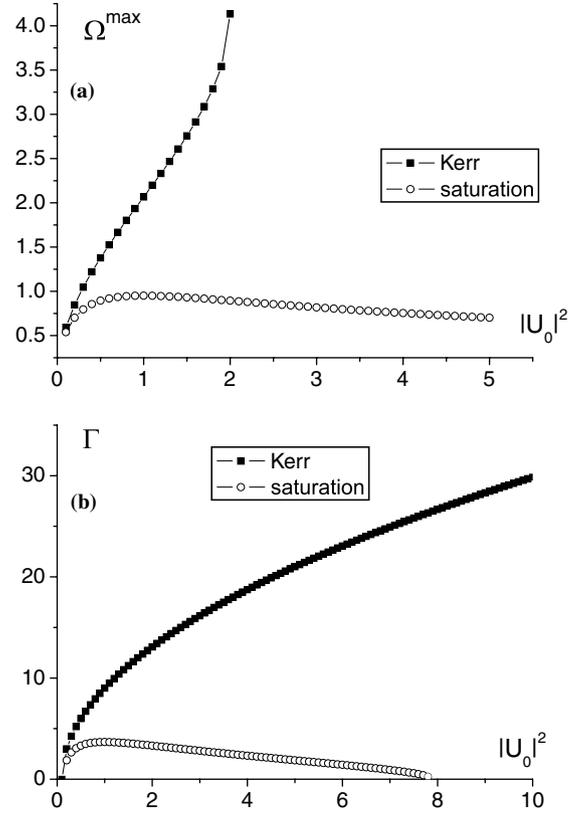

Fig. 5. (a) Critical spatial frequency as a function of the square of the normalized wave amplitude in Kerr case (squares) and in saturable case (circles). Normalized distance between waveguides is $D = 0.76$, while coupling constant is $C = 2.5$, while $\beta = 5$. (b) Gain of perturbation versus the square of the normalized wave amplitude in Kerr case (squares) and in saturable case (circles). Normalized distance between waveguides is $D = 0.76$, coupling constant is $C = 1.5$, $\Omega D = \pi/2$, while $\beta = 15$.

The critical spatial frequency as a function of the square of the normalized beam amplitude in both AlGaAs (squares) and LN NWA's (circles) is shown in Fig. 5a. For a given period of the array and fixed values of both coupling constant and nonlinear coefficient, saturation decreases the critical spatial frequency. In the small amplitude limit, in which Eq. (3) is reduced to Eq. (1), there is indeed almost no difference between these two curves. However, in the region of medium amplitudes, the monotonically growing Kerr curve reaches a maximal value (that is equal to π/D), while the saturable one reaches a corresponding maximum and then slowly decreases in the region of higher amplitudes. A similar behavior has been observed in semiconductor-doped glass fibers [15].

In Fig. 5b we present the dependence of the gain on the square of the beam's amplitude in both arrays. For a given period of the array and fixed values of the spatial frequency of perturbation, nonlinearity, and coupling strength, one can notice that saturation (notation is the same as in Fig. 5a) significantly decreases the MI gain and also restricts the region of amplitudes in which MI can occur. As before, in the small amplitude limit both curves coincide.

Finally, the gain dependence of the spatial frequency of MI for different values of the amplitude and fixed values of

both nonlinearity and coupling strength is given in Fig. 6a and b. As in Figs. 1 and 2, only the positive frequency region is presented. In AlGaAs NWA's (Fig. 6a) the gain diminishes with decrease of the amplitude. In the small amplitude regime, the position of the (critical) spatial frequency for which the gain is maximal moves from the center ($\Omega D = 0$) towards the edges of the perturbation's frequency domain ($\Omega D = \pm\pi$). For very low amplitudes the central region on the x-axis becomes modulationally stable (not presented here). As one can see the relative difference between maximal gain and the gain from adjacent frequencies is quite small especially in the small amplitude regime, where the gain distribution has a wide plateau. As a result, in this region the MI process usually ends up in oscillations [23,30]. Localized structures can be eventually formed in the high amplitude region, where only one frequency with maximal gain can prevail. In LN NWA's (Fig. 6b) gain is significantly smaller compared to the Kerr case and decreases with increase of the beam amplitude. Furthermore, the region of spatial frequencies where this instability may occur diminishes for more intensive beams. Similar as in Refs. [15,40], a degenerate state that evolves from two inputs with different power exists.
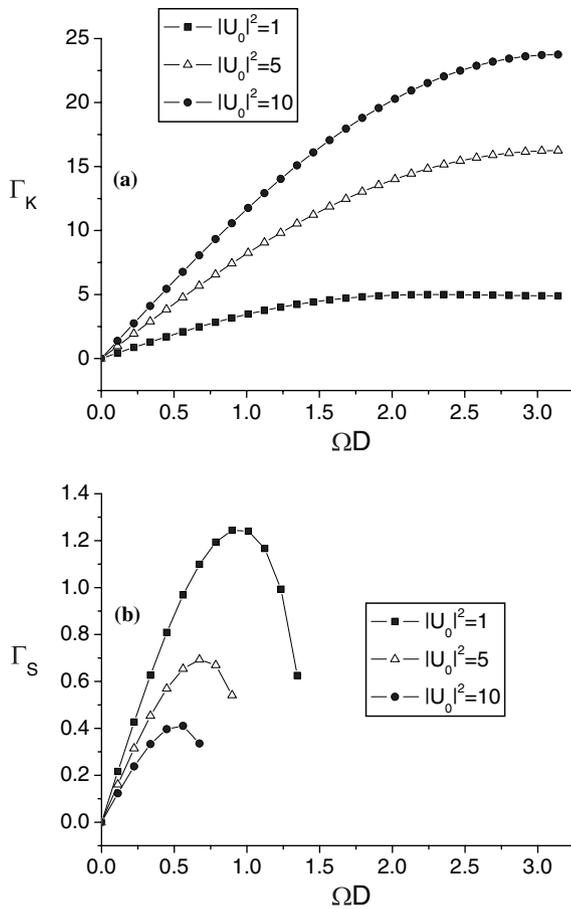
Fig. 6. Dependence of gain on the spatial frequency of the perturbation for different values of the square of the normalized amplitude in (a) Kerr case and (b) in saturable case. System's parameters are $C = 1.5$ and $\beta = 5$.

It is necessary to emphasize that the linear stability analysis which is used to obtain the threshold of instability and corresponding gain is not sufficient to describe the complicated system dynamics after the initial stage of MI [26]. Also, this approach does not take into account possible interactions of the perturbations with the continuous band spectrum which may influence the process of MI. It assumes that this influence may be neglected in the parameter space where a tight-binding approximation is justified. However, as shown on the example of the so-called Dirac-comb nonlinear lattice [44], these interactions could substantially influence the dynamics of MI necessitating a more complete analysis based on a continuous model. Here, it is interesting to mention that one can get Eqs. (7)–(10) no matter which form of perturbations from Refs. [23,24,30] is chosen. For example, if the perturbation from Ref. [30] is taken, one should just replace $\Omega D/2$ with $\pi N/j$ where j denotes the number of humps of the perturbation in the array (in the above mentioned reference $j = 1$ was taken).

4. Conclusion

Modulational instability in one-dimensional discrete media with saturable nonlinearity is studied in detail on the example of permanent channel waveguide arrays in photovoltaic lithium niobate. Instability of wide input staggered beams in such intrinsically self-defocusing media occurs at the edges of the first Brillouin zone where anomalous diffraction is present. Exploiting the fact that the difference between the more accurate Floquet–Bloch approach and the simpler coupled mode approach is small in these regions we have employed the latter one to obtain explicit results for the threshold of instability, maximal spatial frequency, and gain of perturbations. Contrary to the Kerr case, discrete MI in saturable media has a bounded interval of existence. Stronger coupling has an inhibiting role on the MI process, while stronger nonlinearity expedites it. Comparing the corresponding explicit results we demonstrate that saturation stabilizes the frequency region of perturbations around $\pm\pi/2$ and decreases both critical spatial frequency of perturbations and gain. As the cubic DNLS equation is only a small amplitude limit of the saturable DNLS equation these results could be interesting as a generalization of the discrete MI results in the former case. Finally, our results may be useful in investigations of MI in both Bose–Einstein condensates and arrays of Josephson junctions which could be described by similar model equations.

References

[1] R.E. Ergun, C.W. Carlsson, J.P. McFadden, J.H. Clemmons, M.H. Böhm, Geophys. Res. Lett. 18 (1991) 1177.
[2] S.A. Nikitov, S. Jun, R. Marcelli, P. De Gasperis, J. Magn. Magn. Mater. 145 (1995) L6.
[3] J.C. Eilbeck, P.S. Lomdahl, A.C. Scott, Physica D 16 (1984) 318.
[4] M. Stepić, A. Maluckov, Lj. Hadžievski, F. Cheng, D. Runde, D. Kip, Eur. Phys. J. B 41 (2004) 495.
[5] L. Salasnich, A. Parola, L. Reatto, Phys. Rev. Lett. 91 (2003) 080405.
[6] M. Karlsson, J. Opt. Soc. Am. B 12 (1995) 2071.
[7] P.St.J. Russel, J.-L. Archambault, J. Phys. III France 4 (1994) 2471.
[8] D. Kip, M. Soljačić, M. Segev, E. Eugenieva, D.N. Christodoulides, Science 290 (2000) 495.
[9] S. Trillo, P. Ferro, Opt. Lett. 20 (1995) 438.
[10] U. Streppel, D. Michaelis, R. Kowarschik, A. Bräuer, Phys. Rev. Lett. 95 (2005) 073901.
[11] W. Królikowski, O. Bang, J.J. Rasmussen, J. Wyller, Phys. Rev. E 64 (2001) 016612.
[12] R. Schiek, H. Fang, R. Malendevich, G.I. Stegeman, Phys. Rev. Lett. 86 (2001) 4528.
[13] H.P. Wong, Opt. Commun. 213 (2002) 173.
[14] F. Kh. Abdullaev, S.A. Darmanyan, S. Bischoff, M.P. Sørensen, J. Opt. Soc. Am. B 14 (1997) 27.
[15] J.M. Hickmann, S.B. Cavalcanti, N.M. Borges, E.A. Gouveia, A.S. Gouveia-Neto, Opt. Lett. 18 (1993) 182.
[16] N. Da Dalt, C. De Angelis, G.F. Nalesso, M. Santagiustina, Opt. Commun. 121 (1995) 69.

[17] A.B. Aceves, C. De Angelis, S. Trillo, S. Wabnitz, Opt. Lett. 19 (1994) 332.

[18] W. Królikowski, Yu. S. Kivshar, J. Opt. Soc. Am. B 13 (1996) 876.

[19] R.A. Vicencio, M.I. Molina, Yu. S. Kivshar, Opt. Lett. 28 (2003) 1942.

[20] D. Neshev, A.A. Sukhorukov, B. Hanna, W. Królikowski, Yu. S. Kivshar, Phys. Rev. Lett. 93 (2004) 083905.

[21] J. Meier, G.I. Stegeman, D.N. Christodoulides, Y. Silberberg, R. Morandotti, H. Yang, G. Salamo, M. Sorel, J.S. Aitchinson, Opt. Lett. 30 (2005) 1027.

[22] U. Peschel, R. Morandotti, J.S. Aitchinson, H.S. Eisenberg, Y. Silberberg, Appl. Phys. Lett. 75 (1999) 1348.

[23] D.N. Christodoulides, R.I. Joseph, Opt. Lett. 13 (1988) 794.

[24] Yu. S. Kivshar, M. Peyrard, Phys. Rev. A 46 (1992) 3198.

[25] Yu. S. Kivshar, Opt. Lett. 18 (1993) 1147.

[26] J. Leon, M. Manna, Phys. Rev. Lett. 83 (1999) 2324.

[27] J. Meier, G.I. Stegeman, D.N. Christodoulides, Y. Silberberg, R. Morandotti, H. Yang, G. Salamo, M. Sorel, J.S. Aitchinson, Phys. Rev. Lett. 92 (2004) 163902.

[28] M. Chauvet, G. Fu, G. Salamo, J.W. Fleischer, M. Segev, Nonlinear guided waves and their applications topical meeting on CD-ROM, The Optical Society of America, Washington, DC, 2005, WD 39.

[29] M. Peccianti, C. Conti, G. Assanto, A. De Luca, C. Umeton, Nature 432 (2004) 733.

[30] M. Stepić, D. Kip, Lj. Hadžievski, A. Maluckov, Phys. Rev. E 69 (2004) 066618.

[31] A. Maluckov, M. Stepić, D. Kip, Lj. Hadžievski, Eur. J. Phys. B 45 (2005) 539.

[32] M. Stepić, C. Wirth, C.E. Rüter, D. Kip, Opt. Lett. 31 (2006) 247.

[33] R. Iwanow, G.I. Stegeman, R. Schiek, Y. Min, W. Sohler, Opt. Exp. 13 (2005) 7794.

[34] J.-L. Coutaz, M. Kull, J. Opt. Soc. Am. B 8 (1991) 95.

[35] J.M. Hickmann, A.S.L. Gomes, Cid B. de Araújo, Phys. Rev. Lett. 68 (1992) 3547.

[36] S. Nemoto, Appl. Opt. 34 (1995) 6123.

[37] J. McNiff, A.D. Boardman, K. Booth, IEEE Proc. Microw. Antennas Propag. 43 (1996) 189.

[38] B. Luther-Davies, Y. Xiaoping, Opt. Lett. 17 (1992) 496.

[39] P. Dumais, A. Villeneuve, J.S. Aitchinson, Opt. Lett. 21 (1996) 260.

[40] S. Gatz, J. Herrmann, J. Opt. Soc. Am. B 8 (1991) 2296.

[41] A.N. Pikhtin, A.D. Yas'kov, Sov. Phys. Semicond. 14 (1980) 389.

[42] F. Chen, M. Stepić, C.E. Rüter, D. Runde, D. Kip, V. Shandarov, O. Manela, M. Segev, Opt. Exp. 13 (2005) 4314.

[43] K. Peithmann, J. Hukriede, K. Buse, E. Krätzig, Phys. Rev. B 61 (2000) 4615.

[44] A.A. Sukhorukov, Yu. S. Kivshar, Phys. Rev. E 65 (2002) 036609.